

## Clustering at the nuclear surface and symmetry energy

Q. N. Usmani<sup>a\*</sup>, Zaliman Sauli<sup>b</sup> and Nooraihan Abdullah<sup>a</sup>

<sup>a</sup>Institute of Engineering Mathematics, University Malaysia Perlis, Malaysia,

<sup>b</sup>School of Microelectronics Engineering, University Malaysia Perlis, Malaysia

\*qnusmani@hotmail.com

**Abstract.** With in the energy density functional formalism a phenomenological theory of nuclei is developed which incorporates clustering at the nuclear surface in a general form. This explains the large values of symmetry energy extracted recently at low values of nuclear matter density. It is shown that the nuclear matter binding energy per nucleon ( $B/A$ ), in the neighbourhood of zero density, must approach its value at the saturation density. The parameters of the theory are mainly constrained from the binding energies and root mean square radii of 376 spherical nuclei as well as the large values of the recently extracted symmetry energy at low densities. Importance of quartic term in symmetry energy is demonstrated. It is shown that it originates due to clustering as well as due to contribution of three-nucleon interaction in the state-of-the-art equation of state of neutron matter at and below the saturation densities. It is found that clustering significantly reduces the neutron skin thickness in nuclei.

### 1. Introduction

In this contribution, we present the first theory with in the energy density functional (EDF) formalism which includes clustering at the nuclear surface in its most general form. In contrast to earlier theories, for example the Quantum Statistical (QS) approach [1-3] which is based on a generalized Bethe-Uhlenbeck expansion and where only clusters up to  $A \leq 4$  are included, the present approach include clusters of all shapes and sizes along with medium modification. This is achieved in a phenomenological manner. Recently [2,3], large values of symmetry energy has been reported for nuclear matter densities  $\leq 0.009 \text{ fm}^{-3}$  at low temperatures. This arises because of the gain in binding energies due to cluster formation at sub-nuclear densities. Symmetry energy is defined as the difference between energy per nucleon of neutron matter and the nuclear matter. The neutron matter is a super fluid gas with positive pressure at all densities. It follows that the symmetry energy in the vicinity of zero density must approach the nuclear matter binding energy per nucleon as the neutron matter energy goes to zero as density goes to zero. We postulate that the  $B/A$  of nuclear matter at zero density is equal to its value at the saturation density. This follows from the results of virial expansion of the low density nuclear matter which strongly supports the  $\alpha$ -particle clustering [5] as the density and temperature decreases. Also, in an idealized  $\alpha$ -matter calculations, with Coulomb interaction switched off, Johnson and Clark [5], showed that the  $B/A$  of nuclear matter at zero density must approach  $\approx 7.3 \text{ MeV}$ , which is the binding energy per nucleon of the  $\alpha$ -particle without the Coulomb interaction. But why  $\alpha$ -particles? Why not heavier nuclei, or large chunks of nuclear matter itself which would give lower energies as the density approaches zero. In this limit  $B/A$  approaches its value at the saturation density which is around  $16 \text{ MeV}$ , the volume term,  $u_v$ , of the Bethe-Weizsäcker mass formula. This is an exact result. Thus, with the neutron matter  $B/A$  tending to zero with zero density, the symmetry energy at zero density will be equal to  $u_v$ . We incorporate this scenario in an extended

version of the Thomas Fermi theory and investigate its consequences. We address the question, whether the static properties of nuclei, e.g. binding energies and rms radii, are consistent with our postulate of “symmetry energy =  $B/A = u_v$ ” at zero density. Since in nuclei clustering is a surface phenomenon, it will tend to equalize the neutron and proton densities as the  $\alpha$ -particles clustering is expected to be dominant. This may significantly reduce the neutron skin thickness [6]. We find this to be the situation. This has implications for the neutron star studies [7].

The above picture of nuclear matter at low densities is qualitatively different from the one predicted, e.g., from Skyrme-Hartree-Fock (SHF) or Relativistic Mean Field (RMF) theories. The reason is that these theories do not have sufficient correlations to form clusters at the nuclear surface or in the low density nuclear matter. For our purpose, we consider the following thermodynamically consistent picture of nuclear matter as a function of density. At the saturation density, the nuclear matter is nucleonic and stable with  $u_v$  MeV of  $B/A$ . The lower densities of nuclear matter can be envisaged through an isothermal expansion (stretching) with decreasing  $B/A$  as the density decreases due to expansion. Still, the character of NM remains nucleonic and uniform, as is borne out from the accurate auxiliary field diffusion Monte Carlo (AFDMC) calculations [8] with Argonne  $AV_6'$  NN interaction, where  $AV_6'$  is a truncated version of  $AV_8'$  [9]. Further isothermal expansion will eventually bring us to some density where the energy per nucleon will be a maximum and pressure zero, a region of unstable equilibrium. This is the region where cluster formation begins. One can visualize more cluster formation by lowering the density and energy of NM through further expansion; pressure will now be positive in this region. In this region, NM gives away its energy by performing external work. This process can be continued with the formation of larger and larger clusters and binding energies per nucleon till we reach the average zero density. In that limit  $E/A$  again becomes  $-u_v$  MeV and pressure zero. Our equation of state (EoS) for NM adheres to this picture.

In section 2, we give the formulations and show how the above picture of nuclear matter is incorporated in the theory. Section 3 gives the results and discussion. Section 4 is conclusions.

## 2. Formulation

For the EDF we adopt a recent version of Extended Thomas Fermi (ETF) approach. This has been described earlier [10], but it is desirable that we give a few essential details for continuity and more importantly for the crucial required modifications to incorporate clustering at the nuclear surface. The energy of a nucleus is a functional of the density  $\rho$ :

$$E[\rho] = \int \left[ \varepsilon(\rho) + \frac{\hbar^2}{72m} \left( \frac{\nabla \rho}{\rho} \right)^2 + \frac{\hbar^2}{6m} \frac{\nabla^2 \rho}{\rho} + a_\rho \frac{(\nabla \rho)^2}{\rho} \right] \rho d\vec{r} + \int [S(\rho) \delta^2 + Q(\rho) \delta^4] \rho d\vec{r} \quad (1)$$

$$+ \frac{1}{2} e^2 \int \frac{\rho_p(\vec{r}_1) \rho_p(\vec{r}_2)}{|\vec{r}_1 - \vec{r}_2|} d\vec{r}_1 d\vec{r}_2 - \frac{3}{4} \left( \frac{3}{\pi} \right)^{1/3} e^2 \int \rho_p^{4/3}(\vec{r}) d\vec{r} + Shell + a_{pair} \frac{(-1)^Z + (-1)^N}{A^{3/4}}$$

with  $\delta = (\rho_n - \rho_p)/\rho$ . The first integral represents the volume and surface terms. The second integral is the contribution due to symmetry energy and the last two integrals are respectively the direct and exchange Coulomb energy.  $S(\rho)$  and  $Q(\rho)$  shall be described a little later. The term *Shell* is the quantal shell contribution which we extract from Ref [11]. The last term is the pairing energy contribution. Both, the shell and the pairing terms do not play significant roles, as far as the present study is concerned, but they improve the results quantitatively.  $\rho_n$  and  $\rho_p$  are respectively the neutron and proton densities, and  $\rho$  is the total nucleon density;  $\rho = \rho_n + \rho_p$ . We have neglected the deformation effects as we consider only spherical or near spherical nuclei.  $\varepsilon(\rho)$  ( $\equiv E(\rho)/A$ ) is the equation of state of normal nuclear matter.

For  $\varepsilon(\rho)$  we use general density functional. Following Ref. [10], we write it as

$$\varepsilon(\rho_\geq) = -u_v + \frac{K}{18} \left( \frac{\rho - \rho_0}{\rho_0} \right)^2 + M \left( \frac{\rho - \rho_0}{\rho_0} \right)^3, \quad \text{for } \rho \geq \rho_x \quad (2a)$$

$$\varepsilon(\rho_{\leq}) = -u_v + A\rho + B\rho^2 + C\rho^3 + D\rho^4 + \frac{3\hbar^2(3\pi^2)^{2/3}}{5m_N}\rho^{2/3}, \quad \text{for } \rho \leq \rho_x \quad (2b)$$

Notice in 2b, when the density approaches zero, the binding energy per nucleon becomes  $u_v$ . The  $\varepsilon(\rho)$  as given by (2) follows the general pattern for the equation of state of NM as described in the introduction. The constant terms  $A$ ,  $B$ ,  $C$  and  $D$  are determined by equalizing  $\varepsilon(\rho_{\geq})$  and  $\varepsilon(\rho_{\leq})$  and their derivatives at  $\rho = \rho_x$ , where  $\rho_x$  is a density parameter between 0 and  $\rho_0$ .

At present, we have no idea regarding the density dependence of the quartic term in the symmetry energy. We thus assume the same dependence as for the quadratic term and replace  $S(\rho)\delta^2 + Q(\rho)\delta^4$  by  $(1-q)E_{sym}(\rho)\delta^2 + qE_{sym}(\rho)\delta^4$  in (1). The parameter  $q$  determines the relative importance of the two terms. This parameter plays an important role in giving good fit to the binding energies and root mean square radii ( $rms$ ) for our severely constrained EoS of NM and symmetry energy.

An important input in our theory is the neutron matter EoS. For this, we employ the recently calculated values with Argonne  $AV_8'$  [12] and Urbana three-nucleon UIX [13] interactions. This has been obtained by employing an accurate fixed phase AFDMC technique with 66 neutrons enclosed in a periodic box [14]. In Fig. 1 (left panel) we plot the results of Ref. [14], represented by filled circles for  $AV_8' + UIX$ . The solid line is the fit obtained by  $E(\rho)/A = \sum_{i=1,3} y_i \rho_i / (1 + \sum_{i=1,4} y_i \rho_i)$ , where  $y_i$  and  $z_i$  are parameters corresponding to the solid curve. The open circles represent the results with  $AV_8'$  alone and can be obtained by multiplying the solid curve with a fudge factor  $\exp(-2.615(\rho - 0.05))$  for  $\rho > 0.05 \text{ fm}^{-3}$ . We use these fits in our calculations of  $E_{sym}(\rho)$ .

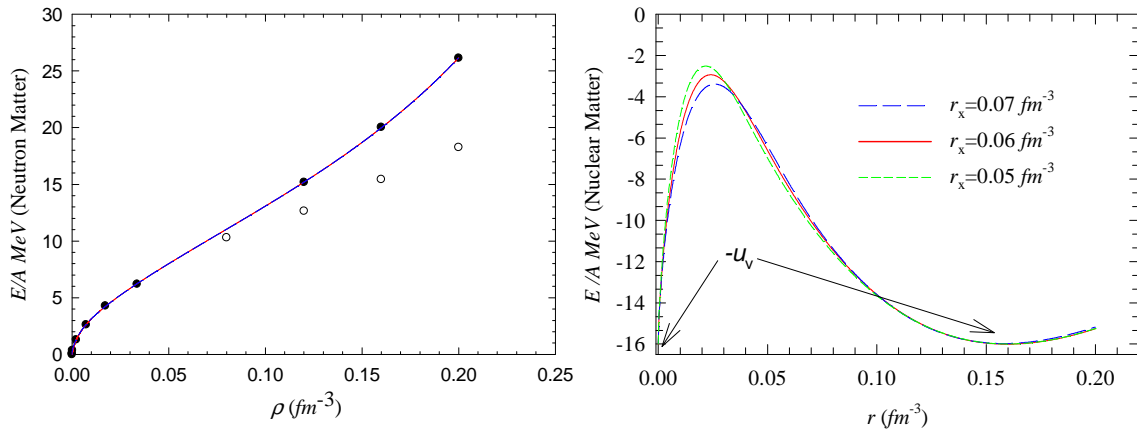


Fig.1: (Color online) Equation of State of neutron and nuclear matter as function of density.

### 3. Results and discussion

We have a total of eight parameters. These are  $K$ ,  $u_v$ ,  $\rho_0$ ,  $M$  and  $\rho_x$  in (2),  $a_\rho$ ,  $q$  and  $a_{pair}$  in (1). We vary seven of them at a time for specific values of  $\rho_x$  to produce the experimental  $rms$  radii [15] and energies [16]. Calculated energies are obtained variationally by varying the density. We have considered 376 spherical nuclei [17-18] from  $^{12}\text{C}$  to  $^{219}\text{U}$ . For the charge  $rms$  radii only 50 nuclei were considered.

rms deviation	Present	Ref. [19]	HFB-17 [16]	LDM+WK[18]	Ref. [17]
$\sigma_E$ MeV	0.937	1.7	0.581	0.630	0.669
$\sigma_R$ MeV	0.023	0.031	0.030	—	—
No. of Nuclei	376	161	2149	367	1654

Table I: Root mean square deviations in various approaches.

In Table 1, we compare our fits with various other approaches. Column 3 gives the result from Ref. [19]. In certain respects, this approach is similar to ours but without incorporating clustering. Column 4, gives the results in the Skyrme-Hartree-Fock-Bogoliubov microscopic-macroscopic approach [20]

but also without clustering. The last two columns, give results for liquid drop models and their various versions with quantal shell corrections and deformation. Considering that we have not included Wigner energy contribution and sophisticated pairing energy terms, as in Refs. [17-18,20], our approach works very well. Our *rms* radii are better than those in the other approaches, though our binding energies are not that good but overall it can be considered satisfactory. In Fig. 2, we plot the differences between the calculated (*cal*) and experimental (*exp*) energies (left panel) and the proton *rms* radii (right panel). These values are plotted for our preferred  $\rho_x = 0.06 \text{ fm}^{-3}$ . We varied  $\rho_x$  between  $0.025$  and  $0.12 \text{ fm}^{-3}$ . The binding energies and *rms* radii are not very sensitive to  $\rho_x$ , but the symmetry energies are. In the right panel of Fig. 1, we plot the EoS for NM for  $\rho_x = 0.05 \text{ fm}^{-3}$  (green, short-dashed curve),  $\rho_x = 0.06 \text{ fm}^{-3}$  (red, solid curve) and  $\rho_x = 0.07 \text{ fm}^{-3}$  (blue, long-dashed curve). For a change of  $\rho_x$  by  $0.02 \text{ fm}^{-3}$ , the change in the location of maximum in the EoS of NM is only  $0.005 \text{ fm}^{-3}$ , which is the region of unstable equilibrium. Thus it is pretty much fixed around  $\rho = 0.026 \text{ fm}^{-3}$  and indicates the onset of clustering around and below this density.

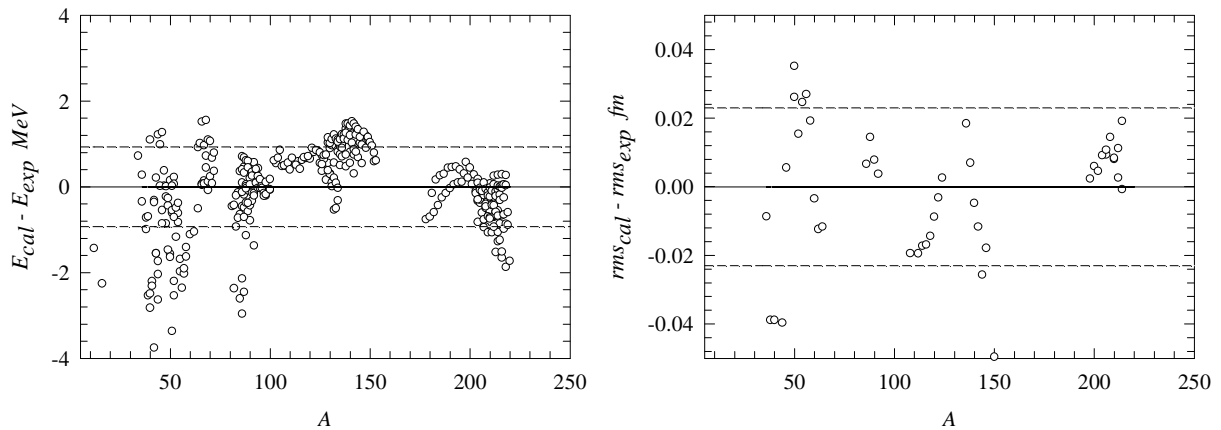


Fig. 2: Calculated and experimental differences for energies and proton charge *rms* radii as a function of *A*.

In Fig. 3, the results for the symmetry energies are given. The color code and legends for the various curves are same as those in Fig. 1 (right panel) described earlier. The dotted curve depicts the results of QS approach [2]. The experimental extraction of the symmetry energy was obtained in Ref. [2,3], in the low density region through heavy ion collisions of  $^{64}\text{Zn}$  on  $^{92}\text{Mo}$  and  $^{197}\text{Au}$  at  $35 \text{ MeV/A}$ . The down blue triangles are the data from [2] which were obtained after correcting it for energy recalibration and reevaluation for particle yields in different velocity bins. They are therefore slightly different from [2]. We have shown an error bar of  $\pm 15\%$  as reported in [3]. Significantly, the medium effects on the clusters play an important role. The up red triangle, are the data from [2] which were corrected for the medium effects in a self consistence way. The whole bunch of data points (down blue triangles) shifts to considerably higher densities (up red triangles) and there is an upward trend for the symmetry energies for lower densities, Fig. 3; the down blue triangles have a downward trend. The slope of our calculated curves, represented by short-dashed, solid and long-dashed lines are all negative at low densities as a result of our ansatz (2) and the EoS of neutron matter. This is in conformity with the data; the up red triangles which have been corrected for medium effects. Clearly, our calculations distinguish between the two sets of data (the up red and down blue triangles). Our symmetry energy shows a distinct minimum at  $\rho_{\text{min}} \approx 0.02 \text{ fm}^{-3}$ . Above this density the quasi-particle picture dominates and below this density the cluster formation takes over. In QS approach, this minimum is not seen, simply because heavier clusters are not included. Thus, it is important that this region of density should be explored experimentally. The right panel of Fig 3 gives an overall picture.

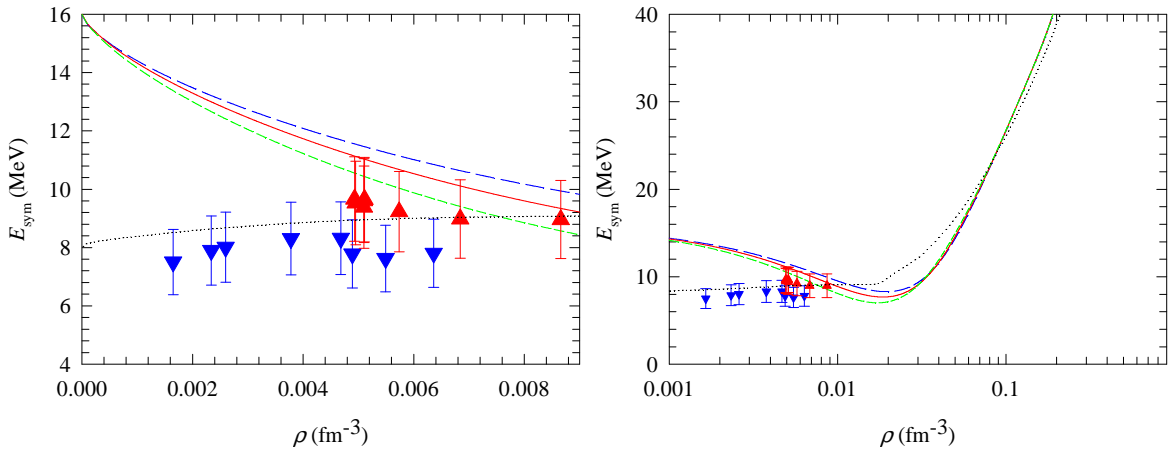


Fig. 3: (Color online) Symmetry energy as function of density. For details, see text.

Neutron Matter	Clustering	$\sigma_E$ MeV	$\sigma_R$ fm	$q$
AV8'+UIX	Yes	7.25	0.080	0.000
AV8'+UIX	Yes	0.937	0.023	0.160±0.004
AV8'+UIX	No	1.368	0.022	0.099±0.006
AV8'	Yes	0.902	0.023	0.076±0.005
AV8'	No	1.290	0.023	0.011±0.005

Table II See text for details.

Appearance of the quartic term in symmetry energy can be attributed to clustering at the nuclear surface and the contribution of three-nucleon interaction near the saturation density in the EoS of neutron matter. We give in table II, fits for various situations pertaining to clustering (Yes,  $u_v \approx 16$  MeV in 2b) and no-clustering (No,  $u_v \approx 0$  MeV in 2b) as well as with and without UIX. Columns 3 and 4 give respectively the root mean square deviations  $\sigma_E$  and  $\sigma_R(rms)$ . In the first row of results, where  $q$  was put equal to zero, *i.e.* no quartic term in the isospin, the  $\sigma$  values are very large. Varying  $q$ , second row, gives a dramatic reduction by a factor of  $\approx 7$  for  $\sigma_E$  and a factor of  $\approx 4$  for  $\sigma_R$ . This amply justifies the inclusion of quartic term and signifies its importance. It is also evident from the results given in the next two rows that both clustering and the three-nucleon interaction in the EoS of neutron matter are responsible for the appearance of the quartic term. The last row roughly mimics the mean field calculations (SHF and RMF). For this and the mean field theories the symmetry energy goes to zero as  $\rho \rightarrow 0$ . Here, there is no clustering, no three-nucleon interaction in EoS of neutron matter and almost no quartic term.

The origin of quartic term due to potential energies at high densities was emphasized in Ref. [21] which we witness here near or below the saturation densities due to three-nucleon interaction as evident from the second and third row of results of table II. The origin of the quartic term due to clustering is perhaps not surprising. The kinetic energy in the symmetry energy are known to have quartic parts, which gets enhanced due to clustering in the low density region. As is also evident from table II, results with clustering are significantly better than with no-clustering.

A quantity of interest is the neutron skin thickness [6], defined as the difference between the *rms* radii of neutrons and protons. In Sky-HF theories  $\delta R$  is sensitive to the slope of the symmetry energy,  $L$ , at the saturation density. We expect the clustering to affect  $\delta R$  significantly as it is a direct surface phenomenon. We find that for  $^{208}\text{Pb}$  and  $^{132}\text{Sn}$ ,  $\delta R = 0.10$  and  $0.16$  fm, respectively. These values are

smaller (by  $\approx 0.05$  fm) as compared to SHF and RMF theories. Our  $L$  value for both the cases of clustering and no-clustering is same;  $L \approx 68$  MeV which is well within the range of values extracted from isospin diffusion data. Our parameter values are, for  $\rho_x=0.06\pm 0.01$ :  $q = 0.16\pm 0.01$ ,  $u_v = 16.00$  MeV,  $\rho_0 = 0.16$  fm<sup>-3</sup>,  $K = 251.55$  MeV,  $M = -8.71\pm 1.50$  MeV,  $a_p = 45.14\pm 0.03$  MeV fm<sup>-5</sup> and  $a_{\text{pair}} = 36.1\pm 1.0$  MeV.

The above considerations will have far reaching consequences for neutron star studies [7] and hypernuclei [22]. For example, due to cluster formation, the  $\Lambda$ -binding to nuclear matter in the neighborhood of zero density must approach to its value at saturation density which is around 30 MeV – an outcome of the conceptual requirement mentioned in the introduction. This indeed is a fundamental departure from all the other earlier approaches and requires a separate study.

#### 4. Conclusions

In conclusion, we have presented a unified theory of nuclei which is reasonably consistent with the static properties of nuclei as well as clustering at the nuclear surface and incorporates the large values of the symmetry energies at low densities. Two main conclusions are: (a) The slope of the symmetry energy is negative at low densities and (b) establishes that quartic term in isospin plays a very important role; it originates from clustering as well as due to three-nucleon interaction. In addition, we have also demonstrated that cluster formation begins for  $\rho$  around  $0.026$  fm<sup>-3</sup> and the symmetry energy has a minimum at  $\rho \approx 0.02$  fm<sup>-3</sup> below which clustering starts dominating.

#### References

- [1] S Typel, G Röpke, T Klähn, D Blaschke and H H Walter, Phys. Rev. C **81**, 015803 (2010).
- [2] J B Natowitz, *et al*, Phys. Rev. Lett. **104**, 202501 (2010).
- [3] S Kowalski *et al.*, Phys. Rev. C **75**, 014601 (2007).
- [4] C J Horowitz and A Schwenk, Nucl. Phys. A **776**, 55 (2006).
- [5] M T Johnson and J W Clark, Kinam **2** 3(1980).
- [6] A R Bodmer and Q N Usmani, Phys. Rev. C **67** 034305 (2003).
- [7] C J Horowitz, J Piekarewicz, Phys. Rev. C **63** 025501 (2001).
- [8] S Gandolfi *et al.*, Phys. Rev. Lett. **98**, 102503 (2007).
- [9] R B Wiringa, V G J Stoks and R Schiavilla, Phys. Rev. **C51** 38 (1995).
- [10] Q N Usmani, A R Bodmer and Z Sauli, C **77**, 034312 (2008).
- [11] W D Myers and W J Swiatecki, LBL Report 36803, 1994; W D Myers, W J Swiatecki, Nucl. Phys., **A 601**, 141 (1996).
- [12] R B Wiringa, V G J Stoks and R Schiavilla, Phys. Rev. **C51** 38 (1995).
- [13] B S Pudliner, V R Pandharipande, J Carlson and R B Wiringa, Phys. Rev. Lett. **74** 4396 (1995).
- [14] S. Gandolfi *et al.*, Phys. Rev. C **79** 054005 (2009).
- [15] I Angeli, Atomic Data and Nuclear Data Tables **87** 185 (2004).
- [16] G Audi, A H Wapstra and C Thibault, Nucl. Phys. **A729** 337 (2003).
- [17] P Möller, J R Nix, W D Myers and W J Swiatecki, At. Data Nucl. Data Tables **59**, 185 (1995).
- [18] A Bhagwat, X Viñas, M Centelles, P Schuck and R Wyss, Phys. Rev. C **81** 044321 (2010).
- [19] M Baldo, P Schuck and X Viñas, Phys. Lett. B **663** 390 (2008).
- [20] S Goriely, N Chamel, and J M Pearson, Phys. Rev. Lett. **102**, 152503 (2009) and references therein.
- [21] Andrew W. Steiner, Phys. Rev. C **74** 045808 (2008).
- [22] R. Sinha, Q. N. Usmani, and B. M. Taib, Phys. Rev. C **66**, 024006 (2002); R. Sinha and Q. N. Usmani, Nucl. Phys. **A684**, 586c (2001); Q. N. Usmani and A. R. Bodmer, Nucl. Phys. **A639**, 147c (1998); Q N Usmani and A R Bodmer, Phys. Rev. C **60**, 055215 (1999); Q. N. Usmani, A. R. Bodmer, and B. Sharma, Phys. Rev. C **70**, 061001 (2004).